

# A series of new conjugated oligothiophenes for organic electronics

Cite as: AIP Conference Proceedings **2257**, 020008 (2020); <https://doi.org/10.1063/5.0023648>  
Published Online: 03 September 2020

Marta Feroci, Tommaso Civitarese, Fabiana Pandolfi, Rita Petrucci, Daniele Rocco, Giuseppe Zollo, and Leonardo Mattiello



View Online



Export Citation

Lock-in Amplifiers  
up to 600 MHz



# A Series of New Conjugated Oligothiophenes for Organic Electronics

Marta Feroci<sup>1</sup>, Tommaso Civitarese<sup>1</sup>, Fabiana Pandolfi<sup>1</sup>, Rita Petrucci<sup>1</sup>, Daniele Rocco<sup>1</sup>, Giuseppe Zollo<sup>1</sup>, Leonardo Mattiello<sup>1,a)</sup>

<sup>1</sup>*Department of Basic and Applied Sciences for Engineering, Sapienza University of Rome, Via del Castro Laurenziano 7, 00161 Rome, Italy*

<sup>a)</sup>Corresponding author: leonardo.mattiello@uniroma1.it

**Abstract.** Thiophene oligomers and polymers can be found in a huge number of materials with applications in the field of Organic Electronics. Chemical and electrochemical syntheses along with electrochemical studies and complete characterization of a series of new conjugated oligothiophene derivatives are reported. Two different molecular architectures, D-A (donor-acceptor) and A-D-A (acceptor-donor-acceptor), were taken into account. The results from voltammetric experiments and optical studies confirm the close relationship between the structure of these compounds and their electrochemical behaviour. This series of oligothiophenes shows low bandgaps, a mandatory requirement for their use in Organic Electronics, and, clearly, they are promising candidates for future synthetic studies in order to modify their optical and electrochemical properties to achieve better performances as organic semiconductors.

## INTRODUCTION

The expression *Organic Electronics* [1] indicates the wide field of materials science regarding the use of organic compounds (small molecules, oligomers [2] or polymers) in electronics. Thiophene ring-containing polymeric [3] and oligomeric [4] derivatives surely are amongst the most utilized organic semiconductor materials. Organic compounds, in general, found a remarkable number of applications as materials used in electronics devices employed in the fields of, *e.g.*: Organic Light-Emitting Diodes (OLEDs) [5], Infrared OLEDs [6], Organic Photovoltaics [7,8], Organic Photodetectors [9], Sensors (for sensing of: natural products [10–12], biomolecules [13], ions in water and food [14], etc.), Organic Field-Effect Transistors [15], and many, many more.

Polythiophenes and oligothiophenes possess from good to excellent charge transport properties and well-established synthetic procedures. Furthermore, in many cases, oligothiophenes show better characteristics (physical, optical, electronic and self-assembly properties, possibility to work in solution, ease of purification, low-cost synthetic procedures) over their polymeric counterparts. In particular, thiophene oligomers possess extended  $\pi$ -electron delocalization along the backbone and are good hole-transporting materials, and they can be synthesized with different architectures in order to fine tuning their optical and electrochemical properties.

We synthesized a series of new conjugated oligothiophenes with two different molecular architectures, donor-acceptor (D-A) and acceptor-donor-acceptor (A-D-A). The oligomers present several cores,  $\pi$ -bridge units and acceptor end groups [4].

In order to obtain a full characterization of organic compounds, optical and electrochemical studies are of crucial importance. One of the best tools, from this point of view, is Cyclic Voltammetry, a technique that permits not only to get insights on reactions pathways and mechanisms [16–20] but also on electrochemical band gaps of organic semiconductors. Nonetheless, the well-known Controlled Potential Electrolysis technique, often utilized in conjunction with cyclic voltammetry, represents a powerful synthetic tool in organic chemistry [21–25].

All the synthesized oligothiophenes were fully characterised and studied by the means of optical and electrochemical techniques [26].

Furthermore, information obtained from Quantum Mechanical Calculations are, in general, extremely useful, and can provide, and predict, for example, optical and electronic properties of the studied compounds [27–34].

Thus, in order to obtain HOMO/LUMO characteristics of some of our novel compounds, quantum mechanical calculations were performed, also with the purpose to confirm our hypotheses based on their electrochemical behaviour [26].

## EXPERIMENTAL SECTION

Unless otherwise stated, starting materials were used as purchased without further purification. Diethyl ether and tetrahydrofuran (THF) were freshly distilled from sodium-benzophenone before use. Reactions were performed under nitrogen atmosphere with standard laboratory equipment and, when required, by the means of a Schlenk apparatus. The catalyst Ni(dppp)Cl<sub>2</sub>, used in the Kumada coupling reactions, was synthesized using published procedures [35]. N-bromosuccinimide (NBS) used in the bromination reactions was purified by the means of standard procedures [36]. The removing of tin by-products (if any) present in the mixtures from stannylation reaction and Stille reaction, were performed by the means of potassium fluoride aqueous solution washings [37]. Thin layer chromatography was carried out using Alugram SIL G/UV254 plates and visualized under UV light (at 254 and/or 365 nm). Flash chromatography was carried out using Silica Gel 60 (0.04-0.063 mm). NMR Spectra and APCI Mass Spectra were previously reported [4]. Quantum mechanical calculations were previously reported [26]. Absorption spectra were measured with a Jasco V-750 double beam spectrophotometer in the 300–800 nm range in a 3 mL cuvette. The samples for UV-Vis spectra were prepared diluting the solution in 2 mL of DCM to obtain an absorbance included in the range 0.1–0.2 at 370 nm. The photoluminescence spectra were measured with a Fluoromax 4 plus (Horiba Yobin Yvon) fluorimeter at the excitation wavelength of 370 nm. The emission interval was maintained constant for all the samples in the 400–700 nm range. Voltammetric experiments were performed using an AMEL System 5000 apparatus. Measurements were carried out, under nitrogen atmosphere, in a conventional three electrode cell with a saturated calomel electrode with multiple junctions as the reference electrode.

## RESULTS AND DISCUSSION

In Figure 1 the two adopted molecular architectures are indicated, each of which consists of different components.

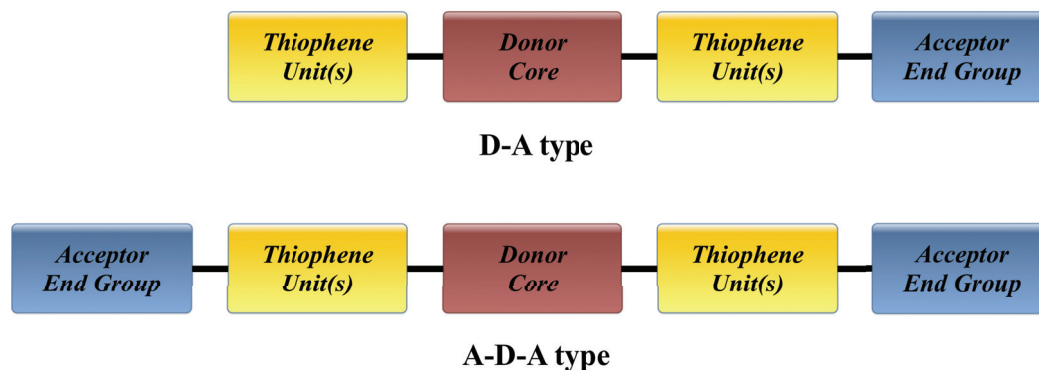
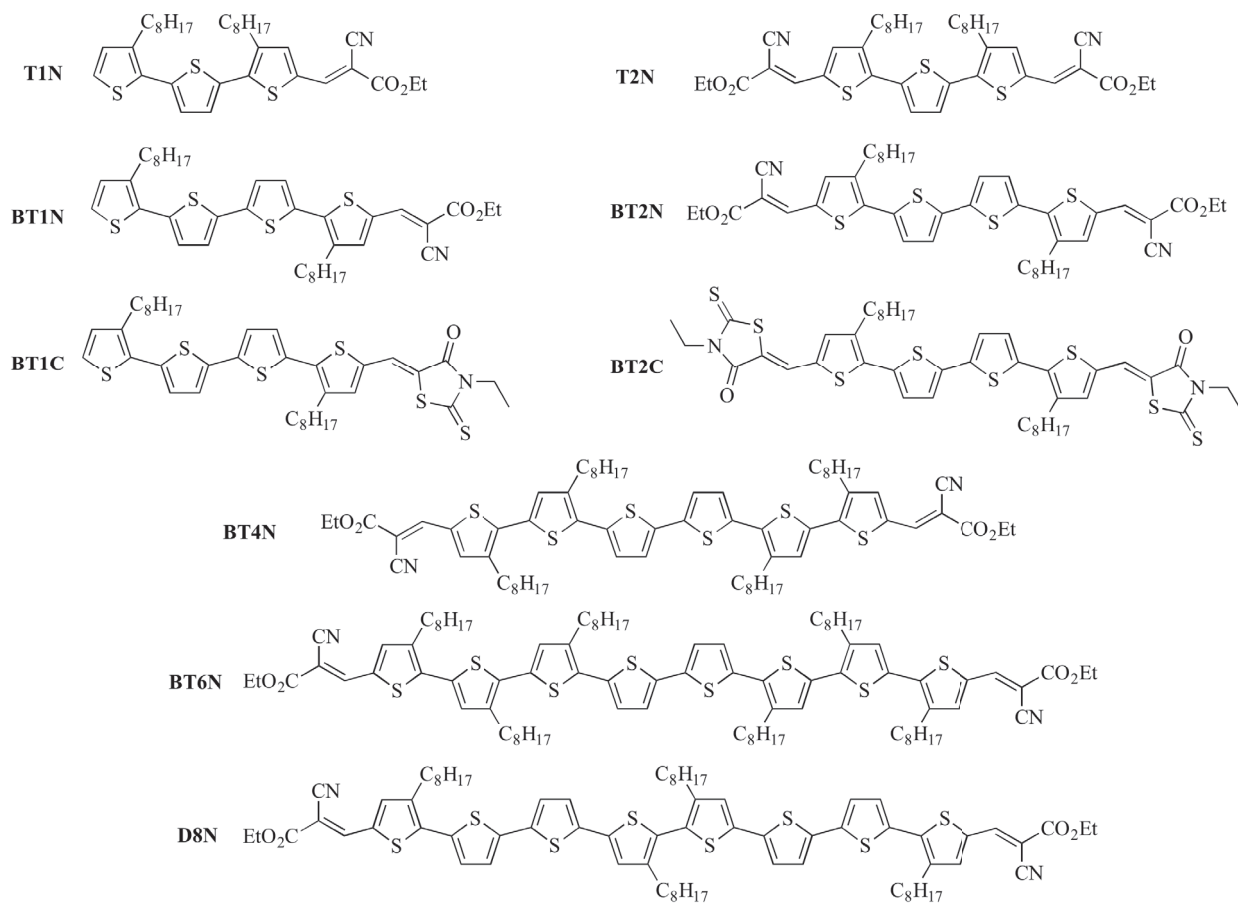


FIGURE 1. D-A and A-D-A type molecular architectures.

The Donor Core consists in thiophene or bithiophene (in the case of oligomer **D8N**, 2,2'-dioctylthiophene). The Thiophene Unit(s) consists in different numbers of 3-octylthiophenes and/or thiophene units (that contribute to the donor part (D) and act as  $\pi$ -bridge and solubilizing components) and the Acceptor End Groups (A) adopted were either ethyl cyanoacrylate or ethylrhodanine units.

In Figure 2 all the newly synthesized oligothiophenes are depicted (only the compound indicated here as **T2N** is a previously reported substance, nevertheless it was also included in our synthetic plan for comparison purposes).



**FIGURE 2.** Structures of all synthesized oligothiophenes.

The chemical syntheses followed different pathways, depending on the target molecules. For better clarity, the synthetic pathways are represented in two different figures.

In Figure 3 the synthetic routes to target compounds **T1N** (ethyl 2-cyano-3-(3,3'-dioctyl-[2,2':5',2''-terthiophen]-5-yl)acrylate) and **T2N** (2,2'-diethyl 3,3'-(3,3''-dioctyl-[2,2':5',2''-terthiophene]-5,5''-diyl)bis(2-cyano-acrylate)) are depicted.

In Figure 4, instead, the syntheses of the tetramers **BT1N** (ethyl 2-cyano-3-(3,3'''-dioctyl-[2,2':5',2''':5''''-quaterthiophen]-5-yl)acrylate), **BT1C** (5-((3,3'''-dioctyl-[2,2':5',2''':5''''-quaterthiophen]-5-yl)methylene)-3-ethyl-2-thioxothiazolidin-4-one), **BT2N** (2,2'-diethyl 3,3'-(3,3'''-dioctyl-[2,2':5',2''':5''''-quaterthiophene]-5,5'''-diyl)bis(2-cyanoacrylate)), **BT2C** (5,5')-5,5'-((3,3'''-dioctyl-[2,2':5',2''':5''''-quaterthiophene]-5,5'''-diyl)bis(methanylylidene))-bis(3-ethyl-2-thioxothiazolidin-4-one), are illustrated.

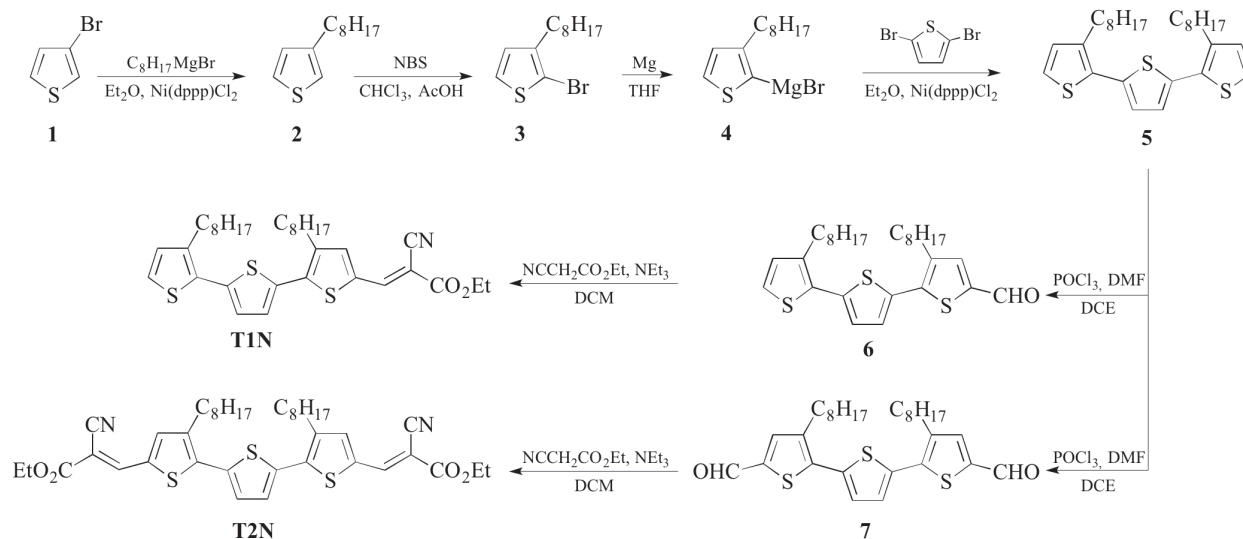


FIGURE 3. Synthesis of trimers **T1N** and **T2N**.

In the cases of the syntheses of the oligomers with three and four thiophene units, the initial step was the synthesis of the “thiophene bridge unit”, namely, the 3-octylthiophene unit (in the form of the Grignard reagent 2-(3-Octylthienyl)magnesium bromide **4**).

This was accomplished starting from the commercially available products 3-bromothiophene **1** and octylmagnesium bromide in order to obtain 3-octylthiophene **2** by the means of a Kumada coupling using, as a catalyst, dichloro[1,3-bis(diphenylphosphino)propane] nickel (II) ( $\text{Ni(dppp)Cl}_2$ ) which was easily synthesized in excellent yields in an open vessel [35]. This catalyst can be stored in anhydrous conditions and remains active for several months.

Then, the bromination of 3-octylthiophene **2** with *N*-bromosuccinimide (NBS) at 0 °C in a chloroform-acetic acid mixture (1:1 v/v) gave 2-bromo-3-octylthiophene **3**, that was, in turn, treated with magnesium in freshly distilled THF in order to give the Grignard reagent 2-(3-Octylthienyl)magnesium bromide **4** that was immediately used in the subsequent Kumada coupling reaction with 2,5-dibromothiophene in order to give the trimer 4,4'-dioctyl-2,2':5',2''-terthiophene **5**.

As previously said, the same synthetic approach was applied also to get the tetramer 3,3''-dioctyl-2,2':5',2''-5,2'''-quaterthiophene **10**, with the only difference that, in order to get a bithiophene central core, instead of 2,5-dibromothiophene, 5,5'-dibromo-2,2'-bithiophene **9** (previously synthesized upon NBS bromination of 2,2'-bithiophene **8**) was used.

The following step was a formylation reaction. Since we were interested, at least for the shorter chain oligomers (three and four thiophene units) to both the formylation adducts, mono- and dialdehyde, we adopted the Vilsmeier-Haack formylation in different experimental conditions (temperature) and different reagents' ratios in order to get both the monoformylated (3,3''-dioctyl-[2,2':5',2''-terthiophene]-5-carbaldehyde **6** and 3,3''-dioctyl-[2,2':5',2''-5,2'''-quaterthiophene]-5-carbaldehyde **11**) and the diformylated (3,3''-dioctyl-[2,2':5',2''-terthiophene]-5,5''-dicarbaldehyde **7** and 3,3''-dioctyl-[2,2':5',2''-5,2'''-quaterthiophene]-5,5'''-dicarbaldehyde **12**) products.

The final step, which gave us the target compounds with the desired D-A and A-D-A molecular architectures, is the Knoevenagel condensation between the formylated oligothiophenes and the precursors of the Acceptor End Groups, ethyl cyanoacetate and 3-ethylrhodanine.

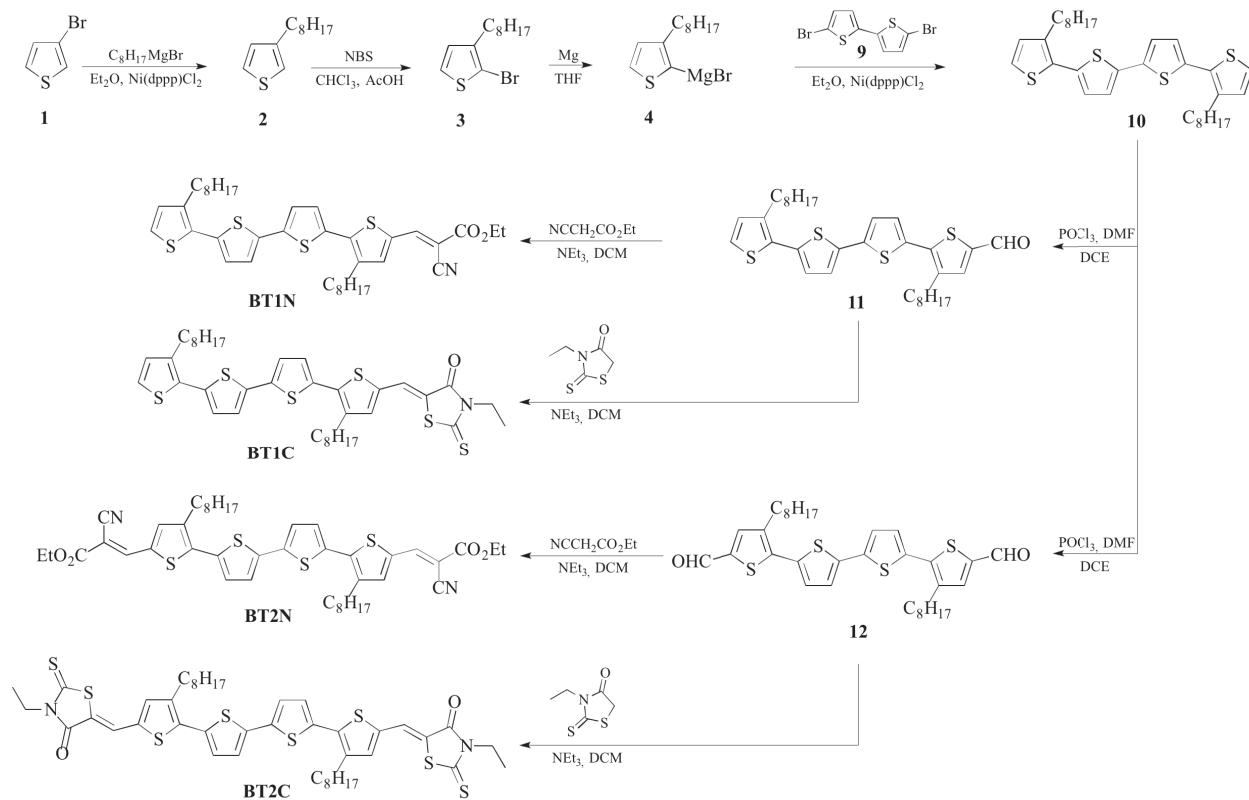


**FIGURE 4.** Synthesis of tetramers **BT1N**, **BT1C**, **BT2N**, **BT2C**.

The synthetic routes adopted in order to obtain the hexamer **BT4N** and the octamer **BT6N**, as previously said, followed different paths compared with their shorter-chain analogues, having in common the use of the Stille reaction, but, nonetheless, again, the two synthetic schemes are separated for better comprehension and clarity and reported in Figure 5 (**BT4N**) and Figure 6 (**BT6N**).

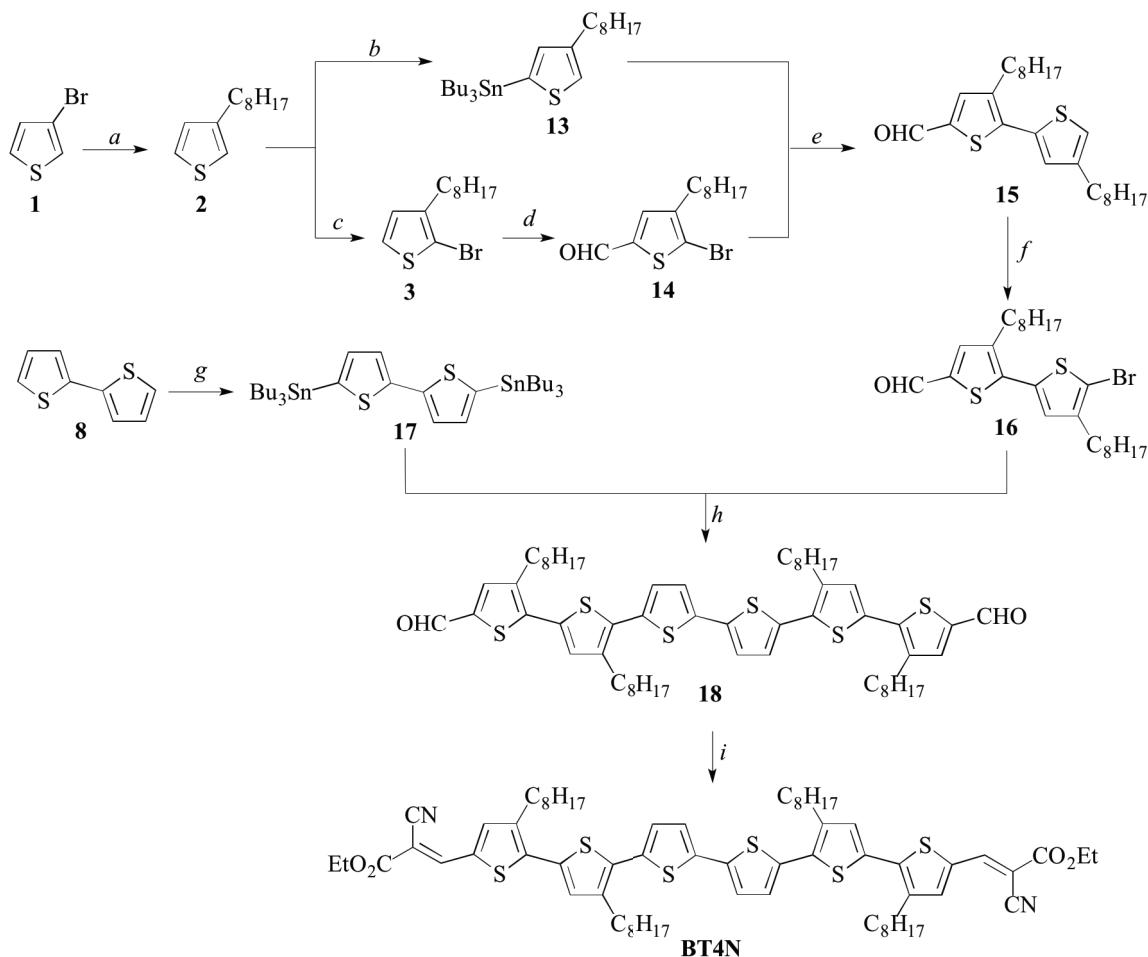


**FIGURE 5.** Synthesis of hexamer **BT4N**. Reaction conditions: *a*) octylmagnesium bromide, Et<sub>2</sub>O, Ni(dppp)Cl<sub>2</sub>; *b*) *n*-BuLi, THF, (Bu)<sub>3</sub>SnCl; *c*) *N*-bromosuccinimide, CHCl<sub>3</sub>-AcOH; *d*) POCl<sub>3</sub>, DMF, 1,2-dichloroethane; *e*) Pd(PPh<sub>3</sub>)<sub>4</sub>, toluene; *f*) *N*-bromosuccinimide, CHCl<sub>3</sub>-AcOH; *g*) *n*-BuLi, THF, (Bu)<sub>3</sub>SnCl; *h*) Pd(PPh<sub>3</sub>)<sub>4</sub>, toluene; *i*) triethylamine, ethyl cyanoacetate, DCM.

The first two synthetic steps adopted to obtain compound **3** were the same used in the synthesis of previous oligomers (Fig. 3 and Fig. 4). Here, compound **3** was then formylated to give 5-bromo-4-octylthiophene-2-carbaldehyde **14**. In this route, starting from the same compound **2** we also synthesized the stannane **13** via a stannylation reaction with tributyltin chloride and *n*-butyllithium at -78 °C, using the obtained crude product without the need of further purification in the following step, *i.e.*, a Stille coupling reaction in dry toluene using tetrakis(triphenylphosphine)-palladium(0) (Pd(PPh<sub>3</sub>)<sub>4</sub>) as the catalyst with the aldehyde **14** in order to get the monoaldehyde **15**.

The latter compound was brominated to give the bromoaldehyde **16**. Another stannylation reaction was needed to synthesize compound **17**. Stannylation and Stille reaction mixtures often are affected by the presence of undesired organotin by-products that need to be removed, with the consequence of a lowering of the yields. The sexithiophene dialdehyde **18** was then obtained as a dark red oil from a Stille coupling reaction between **16** and **17**.

Finally the hexamer **BT4N** was obtained as a black powder by the means of a Knoevenagel condensation.

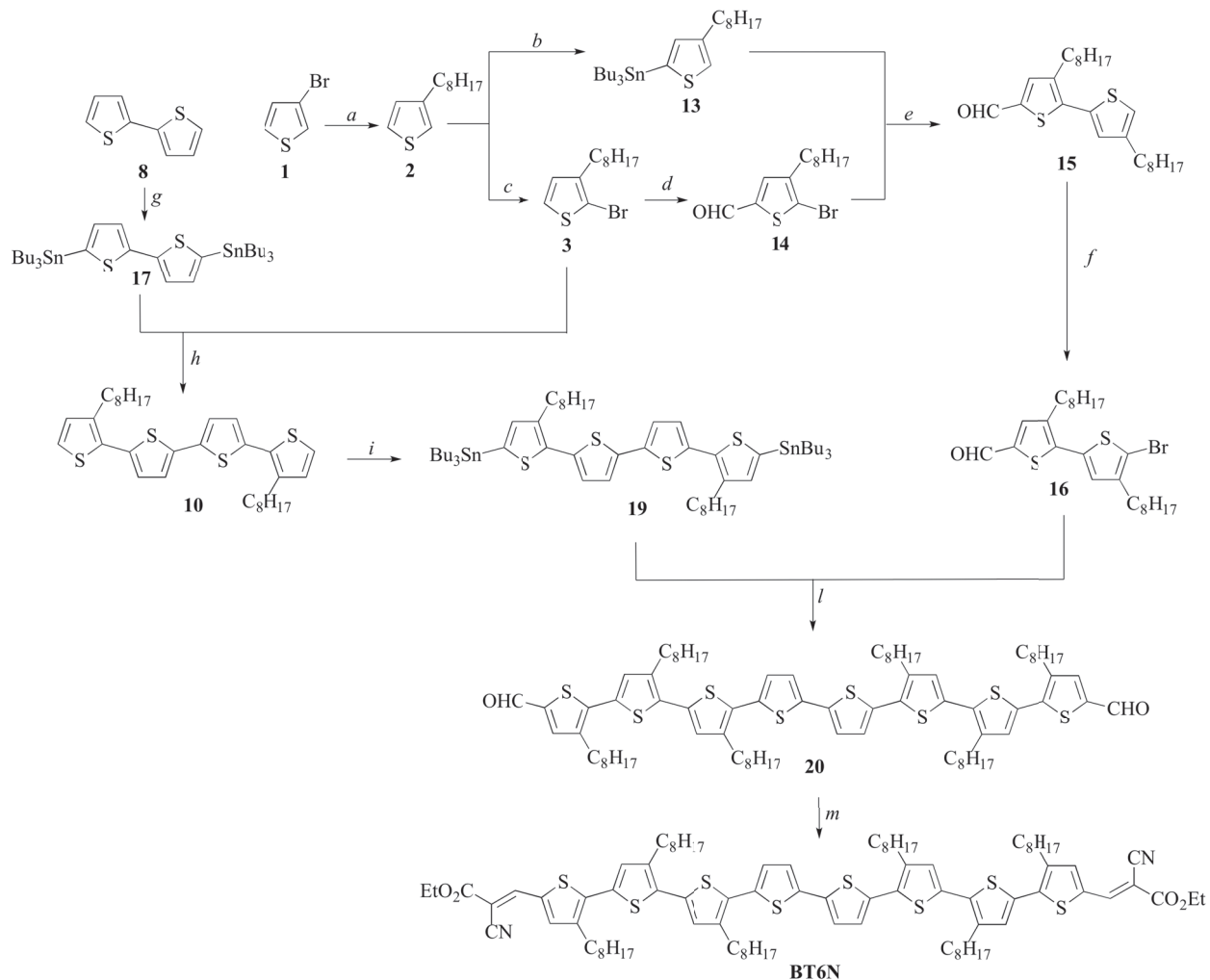


**FIGURE 6.** Synthesis of octamer **BT6N**. Reaction conditions: *a*) octylmagnesium bromide, Et<sub>2</sub>O, Ni(dppp)Cl<sub>2</sub>; *b*) n-BuLi, THF, (Bu)<sub>3</sub>SnCl; *c*) *N*-bromosuccinimide, CHCl<sub>3</sub>-AcOH; *d*) POCl<sub>3</sub>, DMF, 1,2-dichloroethane; *e*) Pd(PPh<sub>3</sub>)<sub>4</sub>, toluene; *f*) NBS, CHCl<sub>3</sub>-AcOH; *g*) n-BuLi, THF, (Bu)<sub>3</sub>SnCl; *h*) Pd(PPh<sub>3</sub>)<sub>4</sub>, toluene; *i*) n-BuLi, THF, (Bu)<sub>3</sub>SnCl; *l*) Pd(PPh<sub>3</sub>)<sub>4</sub>, toluene; *m*) triethylamine, ethyl cyanoacetate, DCM.

In Figure 6, the synthetic passages to compounds **3**, **16** and **17** are the same depicted in Fig. 5. The difference resides in the fact that compound **3** and **17** were coupled by the means of a Stille reaction to give the tetrathiophene **10**, which was, in turn, stannylated to compound **19**. Then, another Stille coupling between compounds **16** and **19** was needed to get the diformyloctithiophene **20**, which was, in turn, subjected to a Knoevenagel condensation to give the octamer **BT6N**, as a black solid.



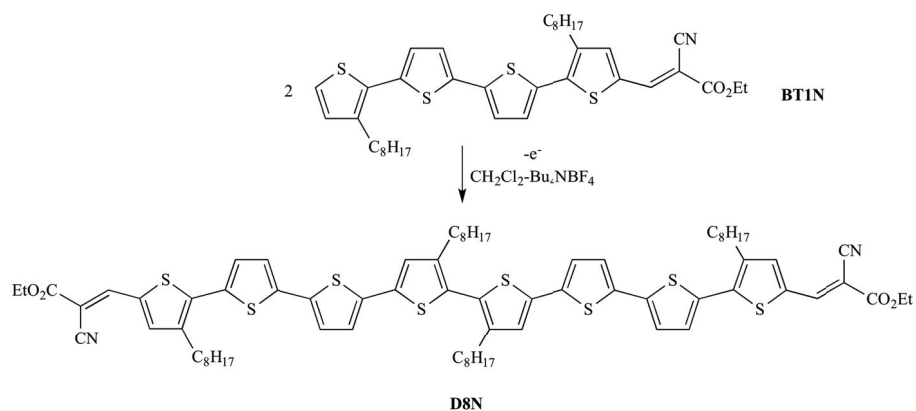


**FIGURE 7.** Synthesis of octamer **DBN** by electrochemical dimerization.

The last compound depicted in Fig. 2 is the octamer **DBN** that was synthesized with a completely different approach, since it was obtained by the means of an electrochemical dimerization [26] of the tetramer **BT1N**, see Figure 7. To our knowledge, no long-chain (>6) oligothiophene was previously synthesized by the means of anodic dimerization and fully characterized. The constant potential electrolysis was performed at 25 °C, in a divided cell; Pt spirals were used as both cathode and anode. DCM- $\text{Et}_4\text{NBF}_4$  0.1 M was used as solvent-supporting electrolyte system under nitrogen atmosphere. The electrolysis potential was +1.2 V (*vs* mSCE).

The optical absorption properties of the synthesized oligothiophenes are reported in Figure 8. Spectra were measured by the means of UV-Vis spectroscopy in dichloromethane solution. All molecules reveal an intense band attributed to the  $\pi\text{-}\pi^*$  transition of the conjugated oligothiophene system. Compound **5**, having as donor core only one thiophene unit, displays a maximum absorption peak ( $\lambda_{\text{max}}$ ) at 338 nm. Changing the central core with 2,2'-bithiophene group, as in compound **10**, causes a red-shift of the  $\lambda_{\text{max}}$  to 379 nm. If an electron withdrawing group is introduced, as an acceptor end unit, it is observed a red-shift of  $\lambda_{\text{max}}$ , depending on the type and number of electron withdrawing groups. In fact, the maximum wavelength is observed for oligothiophene **BT2C** ( $\lambda_{\text{max}} = 508$  nm), that contains two rhodanine moieties as acceptor end groups.

Briefly, the *general trend* points to a red-shift of maximum absorption peaks caused by: the increasing number of thiophene units and/or the change of the molecular architecture from the D- $\pi$ -A type to the A- $\pi$ -D- $\pi$ -A type and/or the change of the end acceptor unit(s), from ethyl cyanoacrylate to (the more powerful electron withdrawing group) ethylrhodanine units.

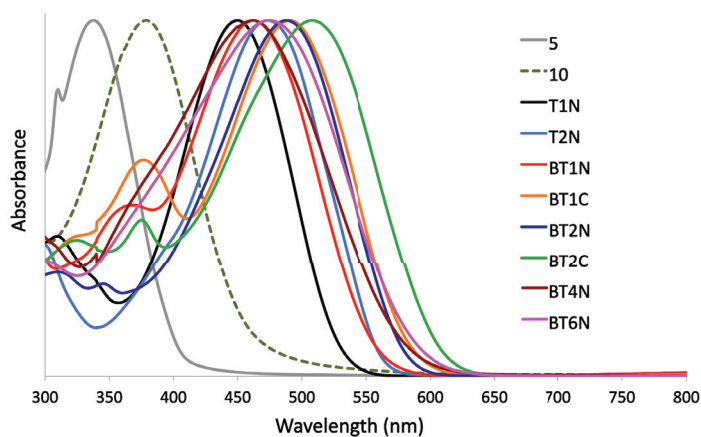


**FIGURE 8.** Normalized optical absorption spectra in DCM solution. Reproduced by permission of The Royal Society of Chemistry from Ref. 4.

The optical emission spectra, in dichloromethane solution, were measured by fluorescence spectroscopy and depicted in Figure 9. In this series of compounds, an evident diminution of the intensity of the emission bands with the extension of the conjugated thiophene backbone can be observed. Moreover, also a red-shift is clearly observed as the number of thiophene units increases. For this reason, for three (out of eight) oligomers it has not been possible the measurement of  $\lambda_{\text{max}}$ , because the maximum emission intensity falls in the infrared region.

All of these results are in accordance with an expected strong intramolecular charge transfer from the thiophene (or bithiophene) donor core to the acceptor end groups.

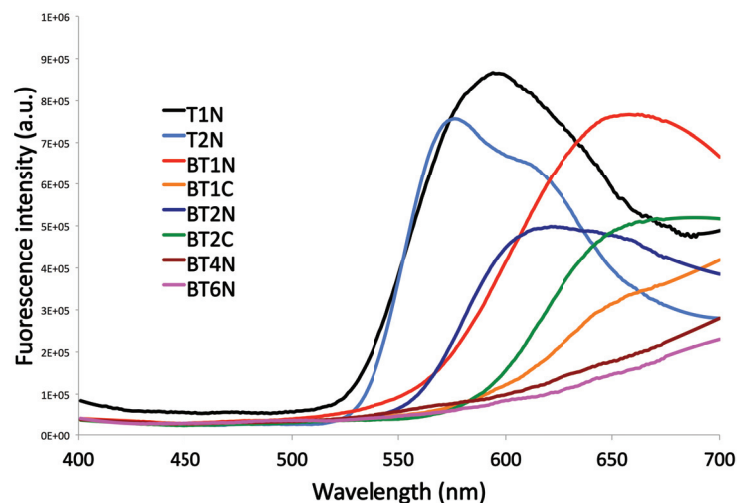


**FIGURE 9.** Fluorescence emission spectra in DCM solution. Reproduced by permission of The Royal Society of Chemistry from Ref. 4.

In order to investigate the energy levels of the synthesized oligothiophenes, cyclic voltammetry technique was used, see Table 1. The energy levels of the highest occupied molecular orbitals and lowest unoccupied molecular orbitals were calculated on the basis of the onset oxidation and reduction potentials [38].

HOMO levels increase from -5.68 to -5.14 eV, following the increase of the length of conjugation, as predictable, in the series **T2N**, **BT2N**, **BT4N** and **BT6N**, *i.e.*, from three to eight thiophene rings, with the same A-D-A architecture and same ethyl cyanoacrylate end groups. Voltammetric data also show that the lowering of the electrochemical bandgaps ( $E_g$ ) is expected on the basis on the same factors taken into consideration observing the optical properties: the kind of donor core, the type of molecular architecture and the acceptor end units.

	$E^{\text{ox}}$ (V)	$E^{\text{red}}$ (V)	$E_{\text{HOMO}}$ (eV)	$E_{\text{LUMO}}$ (eV)	$E_g$ (eV)
T1N	1.14	-0.98	-5.54	-3.42	2.12
T2N	1.28	-0.80	-5.68	-3.60	2.08
BT1N	0.96	-1.00	-5.36	-3.40	1.96
BT2N	1.07	-0.95	-5.47	-3.45	2.02
BT4N	0.82	-0.96	-5.22	-3.44	1.78
BT6N	0.74	-0.94	-5.14	-3.46	1.68
BT1C	0.94	-0.92	-5.34	-3.48	1.86
BT2C	0.90	-0.90	-5.30	-3.50	1.80

**TABLE 1.** Cyclic voltammetry data of chemically synthesized oligomers. The indicated potentials are onset potentials.  $C=1 \times 10^{-3}$  mol  $L^{-1}$ . Solvent system: TBABF<sub>4</sub>/DCM 0.1 mol  $L^{-1}$ . Glassy Carbon electrode, Platinum wire electrode, modified-Standard Calomel reference electrode. Sweep rate = 100 mV  $s^{-1}$ .  $E^\circ(\text{Fc}^+/\text{Fc}) = +0.46$  V vs SCE.

In Figure 10 diluted dichloromethane solutions of some of the synthesized oligothiophenes under UV lighting at 365 nm are depicted, evidencing their fluorescence emission.

The Figure 11, adopting the same colours of Fig. 10 solutions, reports electrochemical bandgaps (eV) of oligothiophene donors vs PCBM, the state-of-the-art acceptor used in photovoltaic devices.

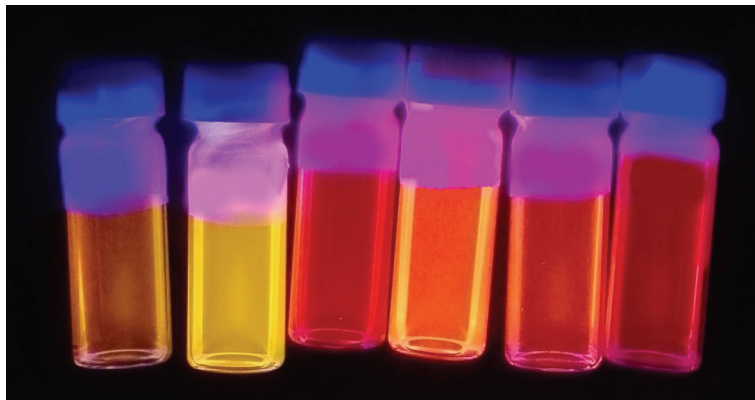


**Figure 10.** DCM solutions of some of the synthesized oligothiophenes under UV light at 365 nm.

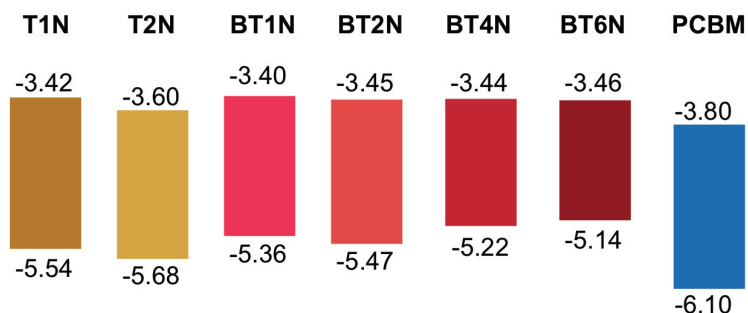


**Figure 11.** Electrochemical bandgaps (eV) of some of the synthesized oligothiophene donors vs PCBM.

## CONCLUSIONS

We synthesized a series of new oligothiophene semiconductors. They differ in the central donor core, in the donor/acceptor architectures and in the acceptor end groups.

The number of thiophene backbone units ranges from three to eight, allowing us to get useful information from their electrochemical and optical properties in correlation with their structures.

Furthermore, the low values of their electrochemical bandgaps associated with their remarkable fluorescence properties make their use promising in different fields of organic electronics.

From this point of view, we thus can consider these new oligothiophenes as candidates for future researches aimed to modify their optical, electrochemical and morphological properties in order to meet the requirements coming from the different fields of applications of organic semiconductors.

## ACKNOWLEDGMENTS

This work was financially supported by Sapienza University of Rome. The authors want to thank Mr. Marco Di Pilato for technical support.

## REFERENCES

1. a) H. Klauk, *Organic Electronics: Materials, Manufacturing and Applications* (Wiley-VCH, Weinheim, 2006); b) H. Klauk, *Organic Electronics II: More Materials and Applications* (Wiley-VCH, Weinheim, 2012).
2. K. Mullen and G. Wegner, *Electronic Materials: The Oligomer Approach* (Wiley-VCH, Weinheim, 1998).
3. L. Salamandra, L. La Notte, G. Paronesso, G. Susanna, L. Cinà, G. Polino, L. Mattiello, A. Catini, C. Di Natale, E. Martinelli, A. Di Carlo, F. Brunetti, T. M. Brown and A. Reale, *Energy Technol.* **131**, 2168–2174 (2017).
4. F. Pandolfi, D. Rocco and L. Mattiello, *Org. Biomol. Chem.* **17**, 3018–3025 (2019).
5. X. Li, J. Zhang, G. Huang, Y. Wang, M. Rong, M. Teng and J. Liu, *Dyes and Pigments* **141**, 1–4 (2017).
6. S. Penna, L. Mattiello, S. Di Bartolo, A. Pizzoleo, V. Attanasio, G. M. Tosi Beleffi and A. Otomo, *J. Nanosci. Nanotechnol.* **16**, 3360–3363 (2016).
7. F. Gala, L. Mattiello, F. Brunetti and G. Zollo, *J. Chem. Phys.* **144**, 084310 (2016).
8. F. Gala, L. Agosta and G. Zollo, *J. Phys. Chem. C* **120**, 450–456 (2016).
9. L. Salamandra, N. Yaghoobi Nia, M. Di Natali, C. Fazolo, S. Maiello, L. La Notte, G. Susanna, A. Pizzoleo, F. Matteocci, L. Cinà, L. Mattiello, F. Brunetti, A. Di Carlo and A. Reale, *Organic Electronics* **69**, 220–226 (2019).
10. R. Petrucci, I. Chiarotto, L. Mattiello, D. Passeri, M. Rossi, G. Zollo and M. Feroci, *Molecules* **24**, 4247 (2019).
11. A. Trani, R. Petrucci, G. Marrosu and A. Curulli "Determination of Caffeine @ Gold Nanoparticles Modified Gold (Au) Electrode: A Preliminary Study", in *Sensors*, part of the Lecture Notes in Electrical Engineering, vol 319 edited by D. Compagnone *et al.* (Springer, Cham, 2015) pp. 147–151.
12. A. Trani, R. Petrucci, G. Marrosu, D. Zane and A. Curulli, *Journal of Electroanalytical Chemistry* **788**, 99–106 (2017).
13. N. Lovecchio, F. Costantini, A. Nascetti, R. Petrucci, G. De Cesare and D. Caputo "Development of an Electrochemiluminescence-based Lab-on-Chip Using Thin/Thick Film Technologies", in *2019 IEEE 8th International Workshop on Advances in Sensors and Interfaces (IWASI)* (IEEE, 2019) pp. 79–83.
14. T. Sun, Q. Niu, Y. Li, T. Li, T. Hu, E. Wang and H. Liu, *Sens. Actuators, B* **258**, 64–71 (2018).
15. C. Zhang and X. Zhu, *Acc. Chem. Res.* **50**, 1342–1350 (2017).
16. M. Feroci, D. Rocco, I. Chiarotto, F. D'Anna, L. Mattiello, F. Pandolfi and C. Rizzo, *ChemElectroChem* **6**, 4275 (2019).
17. I. Chiarotto, L. Mattiello, F. Pandolfi, D. Rocco and M. Feroci, *Front. Chem.* **6**, 7538 (2018).
18. R. Petrucci, G. Zollo, A. Curulli and G. Marrosu, *BBA - General Subjects* **1862**, 1781–1789 (2018).
19. M. Feroci, I. Chiarotto, F. D'Anna, F. Gala, R. Noto, L. Ornano, G. Zollo and A. Inesi, *ChemElectroChem* **3**, 1133–1141 (2016).
20. R. Petrucci, G. Marrosu, P. Astolfi, G. Lupidi and L. Greci, *Electrochimica Acta* **60**, 230–238 (2012).
21. F. Pandolfi, I. Chiarotto, L. Mattiello, D. Rocco and M. Feroci, *Synlett* **30**, 1215–1218 (2019).
22. F. Pandolfi, L. Mattiello, D. Zane and M. Feroci, *Electrochimica Acta* **280**, 71–76 (2018).
23. I. Chiarotto, L. Mattiello, F. Pandolfi, D. Rocco, M. Feroci and R. Petrucci, *ChemElectroChem* **6**, 4511–4521 (2019).
24. D. Rocco, I. Chiarotto, L. Mattiello, F. Pandolfi, D. Zane and M. Feroci, *Pure Appl. Chem.* **91**, 1709–1715, (2019).
25. F. Pandolfi, I. Chiarotto, L. Mattiello, R. Petrucci and M. Feroci, *ChemistrySelect* **4**, 12871–12874 (2019).
26. M. Feroci, T. Civitarese, F. Pandolfi, R. Petrucci, D. Rocco, D. Zane, G. Zollo and L. Mattiello, *ChemElectroChem* **6**, 4016–4021 (2019).
27. F. Buonocore, C. Arcangeli, F. Gala, G. Zollo and M. Celino, *J. Phys. Chem. B* **119**, 11791–11797 (2015).
28. G. Zollo and F. Gala, *Journal of Nanomaterials* **2012**, 1–32 (2012).
29. F. Gala and G. Zollo, *J. Phys. Chem. C* **119**, 7264–7274 (2015).

30. F. Gala and G. Zollo, *Phys. Rev. B* **84**, 195323 (2011).
31. L. Bagolini, F. Gala and G. Zollo, *Carbon* **50**, 411–420 (2012).
32. M. Chinappi, F. Gala, G. Zollo and C. M. Casciola, *Philos. Trans. R. Soc. A* **369**, 2537–2545 (2011).
33. G. Zollo and E. Vitale, *Appl. Sci.* **8**, 2522 (2018).
34. G. Zollo and A. E. Rossini, *Nanoscale Adv.* **1**, 3547–3554 (2019).
35. G. R. Van Hecke and W. D. Horrocks, *Inorg. Chem.* **5**, 1968–1974 (1966).
36. H. J. Dauben Jr. and L. L. McCoy, *J. Am. Chem. Soc.* **81**, 4863–4873 (1959).
37. E. Le Grogneq, J. M. Chrétien, F. Zammattio and J. P. Quintard, *Chem. Rev.* **115**, 10207–10260 (2015).
38. H. Zhang, X. Wan, X. Xue, Y. Li, A. Yu and Y. Chen, *Eur. J. Org. Chem.* **2010**, 1681–1687 (2010).